CORE
Metadata, citation and similar papers at core.ac.uk
Provided by RERO DOC Digital Library

doi:10.1093/brain/aws024 Brain 2012: 135; 1165–1179 | 1165

BRAIN
A JOURNAL OF NEUROLOGY

Altered brain mechanisms of emotion processing in pre-manifest Huntington's disease

Marianne J. U. Novak,[1] Jason D. Warren,[2] Susie M. D. Henley,[3] Bogdan Draganski,[4] Richard S. Frackowiak[4,*] and Sarah J. Tabrizi[3,*]

1 Wellcome Trust Centre for Neuroimaging, University College London Institute of Neurology, Queen Square, London WC1N 3BG, UK
2 Dementia Research Centre, University College London Institute of Neurology, Queen Square, London WC1N 3BG, UK
3 Department of Neurodegenerative Disease, University College London Institute of Neurology, Queen Square, London WC1N 3BG, UK
4 Département des Neurosciences Cliniques, CHUV, University of Lausanne, 1011-Lausanne, Switzerland

*These authors contributed equally to this work.

Correspondence to: Professor Sarah J. Tabrizi,
c/o Box 104,
University College London Institute of Neurology,
Queen Square,
London WC1N 3BG, UK
E-mail: sarah.tabrizi@prion.ucl.ac.uk

Correspondence may also be addressed to: Professor Richard Frackowiak,
Professeur de neurologie,
CHUV BH-10, 46 rue du Bugnon,
1011-Lausanne,
Switzerland
E-mail: Richard.Frackowiak@gmail.com

Huntington's disease is an inherited neurodegenerative disease that causes motor, cognitive and psychiatric impairment, including an early decline in ability to recognize emotional states in others. The pathophysiology underlying the earliest manifestations of the disease is not fully understood; the objective of our study was to clarify this. We used functional magnetic resonance imaging to investigate changes in brain mechanisms of emotion recognition in pre-manifest carriers of the abnormal Huntington's disease gene (subjects with pre-manifest Huntington's disease): 16 subjects with pre-manifest Huntington's disease and 14 control subjects underwent 1.5 tesla magnetic resonance scanning while viewing pictures of facial expressions from the Ekman and Friesen series. Disgust, anger and happiness were chosen as emotions of interest. Disgust is the emotion in which recognition deficits have most commonly been detected in Huntington's disease; anger is the emotion in which impaired recognition was detected in the largest behavioural study of emotion recognition in pre-manifest Huntington's disease to date; and happiness is a positive emotion to contrast with disgust and anger. Ekman facial expressions were also used to quantify emotion recognition accuracy outside the scanner and structural magnetic resonance imaging with voxel-based morphometry was used to assess the relationship between emotion recognition accuracy and regional grey matter volume. Emotion processing in pre-manifest Huntington's disease was associated with reduced neural activity for all three emotions in partially separable functional networks. Furthermore, the Huntington's disease-associated modulation of disgust and happiness processing was negatively correlated with genetic markers of pre-manifest disease progression in distributed, largely extrastriatal networks. The modulated disgust network included insulae, cingulate cortices, pre- and postcentral gyri, precunei, cunei, bilateral putamena, right pallidum, right thalamus, cerebellum, middle frontal, middle occipital, right superior and left inferior temporal gyri, and left superior parietal lobule. The modulated happiness network included postcentral gyri, left caudate, right cingulate cortex, right superior and inferior parietal lobules, and right superior frontal, middle temporal, middle occipital and precentral gyri.

Received July 6, 2011. Revised November 8, 2011. Accepted December 17, 2011
© The Author (2012). Published by Oxford University Press on behalf of the Guarantors of Brain.
This is an Open Access article distributed under the terms of the Creative Commons Attribution Non-Commercial License (http://creativecommons.org/licenses/by-nc/3.0), which permits unrestricted non-commercial use, distribution, and reproduction in any medium, provided the original work is properly cited.

These effects were not driven merely by striatal dysfunction. We did not find equivalent associations between brain structure and emotion recognition, and the pre-manifest Huntington's disease cohort did not have a behavioural deficit in out-of-scanner emotion recognition relative to controls. In addition, we found increased neural activity in the pre-manifest subjects in response to all three emotions in frontal regions, predominantly in the middle frontal gyri. Overall, these findings suggest that pathophysiological effects of Huntington's disease may precede the development of overt clinical symptoms and detectable cerebral atrophy.

Keywords: emotion; Huntington's disease; neurodegenerative disorders; cognitive impairment; functional MRI

Abbreviations: BOLD = blood oxygen level-dependent

Introduction

Huntington's disease is a devastating inherited neurodegenerative disease which causes motor, cognitive and psychiatric impairment. This includes an early and salient decline in the ability to recognize emotional states in others. However, the pathophysiology of emotion processing in Huntington's disease is not fully understood. Improved understanding of emotion recognition difficulties will contribute both to our understanding of Huntington's disease neurobiology, and to the design of symptomatic and disease-modifying therapies. Emotion recognition in Huntington's disease has most frequently been studied by asking subjects to classify pictures of facial expressions by emotion; reduced accuracy is seen in both pre-manifest Huntington's disease gene carriers and patients with manifest disease. Specific findings have, however, been variable, both in behavioural testing (Sprengelmeyer *et al*., 1996, 2006; Gray *et al*., 1997; Wang *et al*., 2003; Hennenlotter *et al*., 2004; Montagne *et al*., 2006; Johnson *et al*., 2007; Henley *et al*., 2008; Aviezer *et al*., 2009; Tabrizi *et al*., 2009) and structural imaging studies (Johnson *et al*., 2007; Kipps *et al*., 2007; Henley *et al*., 2008, 2011). There has been one previous functional MRI study in which emotion perception was tested in Huntington's disease gene carriers: Hennenlotter and colleagues (2004) showed nine subjects with pre-manifest Huntington's disease and nine control subjects pictures of disgusted and surprised (Ekman) faces. Small volume-corrected analyses carried out for regions in the insulae and putamena (based on the results of previous studies in controls) revealed lower levels of blood oxygen level-dependent (BOLD) signal in the left dorsal mid-anterior insula in subjects with pre-manifest Huntington's disease compared with control subjects when they viewed disgusted faces. This finding stimulated our study. We aimed to build on and extend the functional MRI findings of Hennenlotter *et al.* (2004).

The study of emotion processing is of particular interest in Huntington's disease. From a clinical perspective, emotion processing deficits signal disease at an early stage (Johnson *et al*., 2007; Tabrizi *et al*., 2009), while anecdotal accounts from the families of those with Huntington's disease suggest that impaired emotion processing causes relationship breakdown and social isolation. From a pathobiological perspective, emotional stimuli are likely to probe a distributed cerebral network: emotion processing in healthy controls activates widespread brain regions, including the orbitofrontal cortex, amygdalae, basal ganglia and somatosensory cortex (Adolphs, 2001), while Huntington's disease is a whole-brain disease with early regional emphasis in the striatum (Vonsattel *et al*., 1985; Aylward *et al*., 1994; Thieben *et al*., 2002; Rosas *et al*., 2003; Paulsen *et al*., 2006; Tabrizi *et al*., 2009). Neural dysfunction is thought to precede neuronal death and brain atrophy; altered functional profiles during emotion recognition could provide a biomarker of disease evolution. Altered extrastriatal neural activation has previously been detected in subjects with pre-manifest Huntington's disease (Hennenlotter *et al*., 2004; Paulsen *et al*., 2004; Reading *et al*., 2004; Zimbelman *et al*., 2007; Saft *et al*., 2008; Wolf *et al*., 2008; Kloppel *et al*., 2009*a*, *b*).

In this study, we investigated changes in brain mechanisms of emotion recognition in a cohort of subjects with pre-manifest Huntington's disease in order to open a window on Huntington's disease pathophysiology at the earliest stages of disease. Disgust, anger and happiness were chosen as our emotions of interest for the following reasons: disgust is the emotion in which recognition deficits have most commonly been detected across all modalities in Huntington's disease (Calder *et al*., 2010); anger is the emotion in which a recognition deficit was detected in the largest behavioural study of emotion recognition in pre-manifest Huntington's disease to date (Johnson *et al*., 2007); and happiness is a positive valence emotion, in contrast to disgust and anger. We used functional MRI to test the hypothesis that emotion recognition in pre-manifest Huntington's disease is associated with altered neural activation profiles compared with those of healthy controls. We further hypothesized that this altered neural activation would be more anatomically extensive than any disease-related structural changes and would correlate with indices of Huntington's disease gene dosage (CAG repeat length and probability of manifest disease onset within five years). We used structural MRI with voxel-based morphometry to assess the relationship between emotion recognition accuracy and regional grey matter volume.

Materials and methods

Subjects

Sixteen subjects with pre-manifest Huntington's disease (12 female; age 31–65, mean 43.81 years) and 14 age-, sex- and education-matched controls (10 female; age 24–62, mean 39.43 years) were tested. The onset of manifest disease is defined as the point at which characteristic motor signs are seen (1996); our subjects did

not show these signs. The study was approved by the Institute of Neurology's joint University College London/University College London Hospital Trust ethics committee and written informed consent was obtained from every subject. CAG repeat length, quantified through genetic testing, ranged from 39 to 46 repeats in the subjects with pre-manifest Huntington's disease [mean 42, standard deviation (SD) 1.89]. The CAG repeat length was used to estimate the probability of manifest disease onset within the next 5 years for each individual with pre-manifest Huntington's disease (Langbehn *et al*., 2004). This ranged from 0.03 to 0.62 (mean 0.26, SD 0.16). Both CAG repeat length and probability of manifest disease onset within 5 years were tested as they are different markers of Huntington's disease gene dosage: CAG repeat length is invariant from birth, and, as such, can be seen as an overall measure of lifetime gene dosage. Calculation of probability of manifest disease onset within 5 years takes account of an individual's age as well as their CAG repeat length, and therefore is a marker of that individual's gene dosage to date. Probability of manifest disease onset within 5 years can therefore be viewed as a marker of pre-manifest disease progression. Subject demographics are shown in Table 1.

Genetic testing to exclude an expanded *huntingtin* gene was not carried out in the control subjects for ethical reasons (genetic testing has many emotional and practical implications) (Novak and Tabrizi, 2010), but none of the controls were at increased risk above the very small risk in the general population of carrying an expanded *huntingtin* gene.

Behavioural testing

All behavioural testing was carried out after scanning. Explicit recognition of facial expressions of emotion was tested using the Ekman 60 faces test (Young *et al*., 2002) outside the scanner. Executive function was tested using the European Huntington's Disease Network short cognitive battery, which comprises the Stroop task (Stroop, 1935), Symbol-digit modalities test (Smith, 1968), Verbal fluency test (Borkowski, 1967) and Category fluency test (Butters *et al*, 1987); these are sensitive to cognitive decline in manifest Huntington's disease. Premorbid intelligence was estimated using the National Adult Reading Test (Nelson and Willison, 1991). Visual perception of facial identity was tested using the Benton Facial Recognition Test (Benton *et al*, 1983). Formal depression scores were not obtained, but all subjects were tested and debriefed by a clinician with experience in Huntington's disease (M.J.U.N.); no significant evidence of clinical depression was detected.

Functional magnetic resonance imaging task

During scanning, subjects viewed Ekman and Friesen pictures of facial affect (Ekman *et al*., 1976) which had been cropped to remove hair and facial outline. While viewing the faces, subjects carried out a distractor task of categorizing each face by gender with a button press; implicit processing of facial expressions of emotion was therefore tested in the scanner. A block design was used with the following four block types: disgusted, angry, happy and neutral faces. Each block consisted of 10 different faces showing the same facial expression. Each face was shown for 1 s, with a 0.5–1.5 s jitter between them. Neutral faces were a morph of 75% neutral face and 25% happy face [since 100% neutral faces are often perceived as adversarial (Hennenlotter *et al*., 2004)]. Each block was shown four times; there were 16 blocks in total, shown in pseudorandomized order.

Table 1 Clinical and neuropsychological characteristics of subjects

	Age	CAG repeat length	Probability of manifest disease onset within 5 years	National Adult Reading Test	Years of full time education	Unified Huntington's disease Rating Scale motor score	Stroop colour	Stroop word	Stroop interference	Symbol -digit modalities test	Category fluency	Verbal fluency	Benton facial recognition score	Ekman 60 faces test		
														Anger	Disgust	Happiness
Mean (SD) in Huntington's disease group	43.81 (8.30)	42 (1.89)	0.26 (0.16)	36.13 (6.69)	15.88 (3.46)	4.93 (6.57)	88.36 (27.00)	108.57 (18.10)	50.07 (14.94)	58.07 (14.74)	30.2 (19.52)	16.36 (4.62)	40.27 (13.54)	8.19 (1.68)	7.69 (1.89)	9.88 (0.34)
Mean (SD) in control group	39.43 (11.40)	n/a	n/a	35.07 (8.56)	15.86 (3.23)	0.31 (0.63)	83.14 (11.98)	106.5 (14.75)	51 (11.56)	63.93 (11.90)	27.54 (5.16)	14.79 (2.89)	47.57 (4.31)	8.79 (1.12)	7.71 (2.16)	10 (0)
Two tailed t-test (P-value; *equal variance; **unequal variance)[a]	0.23*	n/a		0.71*	0.99*	0.02**	0.51*	0.74*	0.86*	0.26*	0.64*	0.28*	0.06*	0.27*	0.97*	0.18*

[a]Homogeneity of variance tested with Levene's test ($P < 0.05$).
Fisher's exact test showed no difference in gender distribution between the groups ($P = 0.574$).

Table 2 Details of functional MRI models

Model number	Subject groups	Covariates
1	Control and pre-manifest Huntington's disease	None
2	Control and pre-manifest Huntington's disease	CAG repeat length or probability of manifest disease onset within 5 years
3	Pre-manifest Huntington's disease only	CAG repeat length or probability of manifest disease onset within 5 years, age, gender
4	Pre-manifest Huntington's disease only	Disgust only: mean striatal BOLD signal, age, gender
5	Control and pre-manifest Huntington's disease	Ekman 60 out-of-scanner score

Brain image acquisition

Subjects were scanned on a Siemens 1.5T Sonata MRI scanner (Siemens Medical Systems). Echo planar imaging data were acquired during the functional MRI task using the following scanning parameters: repetition time = 4.32 s, slice repetition time = 90 ms, echo time = 50 ms, flip angle = 90°, distance factor = 50%, voxel size 3 × 3 × 3 mm (Weiskopf *et al.*, 2006). Forty-eight slices of 2 mm thickness were acquired and the sequence was selected to achieve optimal whole-brain coverage. The first five 'dummy' volumes were discarded to allow for T_1 equilibration effects. Field inhomogeneity maps were also acquired. A T_1-weighted whole-brain structural image was acquired for every subject with pre-manifest Huntington's disease and 13 of the controls. One hundred and seventy-six slices of 1 mm thickness were acquired with the following parameters: repetition time = 20.66 ms, echo time = 8.42 ms, flip angle = 25°, slice thickness = 1 mm, 176 slices, voxel size 1 × 1 × 1 mm (Deichmann, 2006).

General principles of data analysis

All data were first analysed at a group level by comparing pre-manifest Huntington's disease and control data. Parametric analyses of the pre-manifest Huntington's disease data alone were then carried out to assess relationships between functional changes and Huntington's disease metrics (CAG repeat length and probability of manifest disease onset within 5 years).

Imaging data analysis

MRI data were processed using Statistical Parametric Mapping software (SPM8; Wellcome Trust Centre for Neuroimaging http://www.fil.ion.ucl.ac.uk/spm) run on a MATLAB 7 R2010 platform (MathWorks).

Functional magnetic resonance imaging data

Functional data were spatially realigned then corrected for inhomogeneity artefacts using the reconstructed field maps. They were then registered to the standard Montreal Neurological Institute space using the echo planar imaging template provided in SPM8, and finally smoothed with a 10 mm full-width half-maximum Gaussian kernel. Statistical analysis was carried out using the general linear model (Friston *et al.*, 1995). Each block of data was modelled as a boxcar function and convolved with the canonical haemodynamic response function and its temporal derivative to create a regressor of interest. Four regressors of no interest were modelled: button press times that followed presentation of a stimulus, additional (erroneous) button press times, stimulus presentation times of those trials where no button response was made and the subject-specific movement parameters. Three effects of interest were modelled in a common first level design matrix: each emotion regressor was compared with the neutral regressor in the following contrasts: (disgust > neutral), (anger > neutral) and (happiness > neutral).

Parameter estimates for these conditions were estimated at every voxel for each subject and then entered into a second level random effects analysis. A series of models was assessed at the second level to explore the effects of potentially relevant disease-associated factors; these models are summarized in Table 2.

Three models were initially created for each condition: two factorial models to compare the control and pre-manifest Huntington's disease groups (Table 2, Models 1 and 2), and one regression model, which contained data from the pre-manifest Huntington's disease group only (Table 2, Model 3). The first factorial model contained no additional regressors, whereas the second factorial model contained mean-corrected CAG repeat length and probability of manifest disease onset within five years respectively as regressors of 'no interest', or 'nuisance covariates'. The second model therefore enabled us to test for differences in mean activation levels between the pre-manifest Huntington's disease and control groups after controlling for heterogeneity in the pre-manifest Huntington's disease data accounted for by CAG repeat length and probability of manifest disease onset within 5 years. As there is no evidence that CAG repeat length modulates behaviour at non-pathogenic repeat lengths, the controls were all allotted CAG repeat length (and probability of manifest disease onset within 5 years) values of zero, i.e. we used a constant regressor to model the data with the assumption that variability in the control data could not be attributed to CAG repeat length, in contrast to that in the pre-manifest Huntington's disease data. The pre-manifest Huntington's disease and control groups were matched for age and sex; these were not therefore entered as regressors in between-group comparisons. When pre-manifest Huntington's disease data only were included in the design matrix, age and sex were added as 'nuisance covariates'. Benton facial recognition score was added as a 'nuisance covariate' in all models, in order to account for another relevant cognitive capacity (face perception) that may have influenced facial emotion processing. The pre-manifest Huntington's disease regression models contained CAG repeat length and probability of manifest disease onset within 5 years as additional regressors.

A second set of analyses was carried out to assess whether altered extrastriatal activation in the pre-manifest Huntington's disease group was driven primarily by altered striatal activation (Table 2, Model 4). A bilateral caudate/putamen/pallidum region of interest was defined using the WFU PickAtlas (Maldjian *et al.*, 2003, 2004). For the pre-manifest Huntington's disease regression model that showed the most anatomically extensive correlations (disgust > neutral), the mean beta value (an index of BOLD activity) of voxels within the caudate/

putamen/pallidum region of interest was calculated for each subject. These mean striatal values were then re-entered into the corresponding model as an additional regressor. A mask of the significant voxels from the original analysis was applied (voxels in which a significant inverse association between CAG repeat length and neural activity was seen), and correlations between the mean striatal values and extrastriatal activity were calculated in order to identify extrastriatal voxels in which the BOLD signal covaried with the mean striatal BOLD signal.

Finally, a third set of analyses was carried out to assess the relationship between the BOLD signal during emotion processing and accuracy scores from the previously described out-of-scanner Ekman 60 tests (Table 2, Model 5). These analyses were carried out to assess differences between the pre-manifest Huntington's disease and control subjects in the extent to which anatomical associations of emotion processing were related to the behavioural measure of emotion recognition by adding the Ekman 60 scores into the models for the corresponding emotion as regressors of interest.

Whole-brain analyses were carried out for every contrast. Results are reported using set level significance $P < 0.05$; set level significance was chosen because emotion recognition tasks and Huntington's disease itself were predicted to produce changes in distributed neural networks rather than in discrete brain regions (Friston *et al*., 1996). Height threshold was set at $P < 0.01$; cluster size threshold at $\geqslant 20$ voxels.

Debriefing of our subjects after scanning revealed that all became aware of the emotional content of the stimuli over the course of the experiment. Additional *post hoc* analyses were therefore carried out to compare BOLD levels in the first blocks of the experiment (during which most subjects were not yet aware of the emotion content) with the BOLD levels in the final blocks (during which all subjects were aware that different blocks contained different emotional stimuli).

Structural imaging data

Structural MRI data were first partitioned into three tissue classes—grey matter, white matter and CSF—using the 'unified segmentation approach' in SPM8 (Ashburner and Friston, 2005). The grey matter maps were registered to the standard Montreal Neurological Institute space using Dartel, a diffeomorphic registration algorithm (Ashburner, 2007), adjusted for linear and non-linear effects of normalization (i.e. 'modulated'), and then smoothed with a 10 mm full-width at half-maximum Gaussian kernel. This produced smoothed modulated normalized grey matter data which were statistically analysed using a general linear model; this generated a voxelwise comparison of local tissue volumes (Ashburner and Friston, 2000). General linear models were also constructed to look for interactions between regional grey matter volume and out-of-scanner Ekman 60 test scores in the pre-manifest Huntington's disease group versus controls. Total grey matter volume was entered as an additional regressor in the design matrix to control for variance in overall brain size so that regional grey matter volume changes were identified. Whole-brain atrophy rates in Huntington's disease gene carriers are higher than those in controls (Henley *et al*., 2009); by controlling for overall grey matter volume, we therefore sought specifically to identify regional grey matter volume loss over and above total grey matter volume loss. A non-stationarity correction (Hayasaka *et al*., 2004) was used to correct for non-uniformity in smoothness, allowing for the use of cluster-based significance values. Statistical parametric maps were thresholded at the cluster level using family-wise error correction for multiple comparisons at $P < 0.05$.

As in the functional MRI analyses, age and sex were not entered as regressors in between-group comparisons, but were included in pre-manifest Huntington's disease-only analyses. Separate pre-manifest Huntington's disease models were constructed with CAG repeat length and probability of manifest disease onset within 5 years as regressors of interest to test their relationship with regional grey matter volume. Whole-brain structural analyses were followed by region of interest analyses; the regions of interest were based on prior anatomical hypotheses concerning the brain substrates for emotion processing and the evolution of atrophy in Huntington's disease, and were defined using the WFU PickAtlas (Maldjian *et al*., 2003, 2004). These regions of interest were combined and used to reduce the search volume to caudate, putamen, pallidum, insula, amygdala, somatosensory cortex and orbitofrontal cortex by applying small volume correction (Worsley *et al*., 1996). In addition, a bilateral caudate/putamen/pallidum-only region of interest was used for those analyses not involving emotion data; the regions were chosen to reflect the predominance of early structural Huntington's disease changes in these nuclei.

Results

Behavioural data

Out-of-scanner behavioural data are summarized in Table 1 (a breakdown of the results for individual subjects is available from the authors on request). The pre-manifest Huntington's disease and healthy control groups did not differ in accuracy for recognition of disgust, anger or happiness (happiness recognition was near ceiling level across both groups), whether or not CAG repeat length and probability of manifest disease onset within 5 years were adjusted for (ANCOVA, $P > 0.05$). Scores in the group with pre-manifest Huntington's disease were normally distributed only for disgust recognition (Kolmogorov-Smirnov test, $P > 0.05$), so Spearman's correlation coefficient (one-tailed) was used to assess correlations between Ekman scores and CAG repeat length and probability of manifest disease onset within 5 years. In the pre-manifest Huntington's disease group, accuracy of disgust recognition was found to correlate inversely with CAG repeat length (Spearman's correlation coefficient = -0.635), and accuracy of anger recognition inversely with CAG repeat length (Spearman's correlation coefficient = -0.466) and probability of manifest disease onset within 5 years (Spearman's correlation coefficient = -0.529) ($P < 0.05$). There was no difference in task performance between the groups on the European Huntington's Disease Network short cognitive battery, the National Adult Reading Test or the Benton facial recognition test. Subjects with pre-manifest Huntington's disease had significantly higher scores than controls on the Unified Huntington's Disease Rating Scale motor score ($P = 0.02$; pre-Huntington's disease score range = 0–24; control score range = 0–2); the effects of subtle motor impairment in the subjects with pre-manifest Huntington's disease were controlled for in the functional MRI analyses by including button press times (i.e. reaction times) as regressors in the first level models.

Functional magnetic resonance imaging data

Functional MRI results are reported in three sections: (i) and (ii) analyses using models that contained no data about out-of-scanner emotion recognition accuracy (Table 2, Models 1–4; showing the neural substrates of emotion processing in pre-manifest Huntington's disease) and (iii) analyses using models that included a regressor containing the Ekman 60 recognition score for the corresponding emotion (Table 2, Model 5; showing the relationship between neural activity and behaviour on the out-of-scanner Ekman 60 test). Results are reported with set level significance $P < 0.05$. Regional anatomical data are summarized in Table 3; statistical parametric maps are displayed overlaid on a mean structural image in Figs 1 and 2 and Supplementary Figs 4–6. In the *post hoc* analyses investigating systematic alterations in BOLD response over time in the scanner (i.e. BOLD effects potentially associated with a qualitatively altered mode of cognitive processing of the emotion stimuli over the course of the experiment), no trends were seen.

(i) Models testing for differences in activation between the pre-manifest Huntington's disease and control groups (not including the Ekman 60 regressor)

After adjusting for variance in the pre-manifest Huntington's disease group attributable to gene dosage by adding CAG repeat length and probability of manifest disease onset within 5 years respectively as 'nuisance variables' (Table 2, Model 2), extensive regions were found in which controls had greater activation than the pre-manifest Huntington's disease group in all three emotion contrasts: the disgust > neutral condition (with CAG repeat length correction, $P < 1 \times 10^{-10}$; nine clusters; with probability of manifest disease onset within 5 years correction, $P < 1 \times 10^{-10}$; 17 clusters), the anger > neutral condition (with CAG repeat length correction, $P < 1 \times 10^{-10}$; nine clusters; with probability of manifest disease onset within 5 years correction, $P < 1 \times 10^{-10}$; seven clusters), and the happiness > neutral condition (with CAG repeat length correction, $P < 1 \times 10^{-10}$; 11 clusters; with probability of manifest disease onset within 5 years correction, $P < 1 \times 10^{-10}$; 12 clusters).

The network of decreased activation identified in the disgust > neutral contrast after CAG repeat length adjustment included right middle frontal gyrus, left precentral gyrus, right postcentral gyrus, bilateral paracentral lobules, left anterior and mid-insula, left superior and inferior parietal lobules and right posterior cingulate cortex. Similar results were seen with probability of manifest disease onset within 5 years replacing CAG repeat length in the model (Table 2, Model 2).

The network of decreased activation identified in the anger > neutral contrast after CAG repeat length adjustment included right caudate, left paracentral lobule, bilateral anterior and mid-insulae, bilateral hippocampi, left middle occipital gyrus and right mid-cingulate cortex (Table 2, Model 2). Similar results were seen with probability of manifest disease onset within 5 years replacing CAG repeat length in the model.

The network of decreased activation identified in the happiness > neutral contrast after CAG repeat length correction included bilateral caudates, left precuneus, right anterior and mid-insula, left hippocampus, left cuneus, bilateral middle occipital gyri and bilateral anterior cingulate cortex. Similar results were seen with probability of manifest disease onset within 5 years replacing CAG repeat length in the model (Table 2, Model 2).

After adjusting for variance in the pre-manifest Huntington's disease group attributable to gene dosage (Table 2, Model 2), regions were also found in which the subjects with pre-manifest Huntington's disease had greater activation than the controls in the disgust > neutral (with CAG repeat length correction, $P = 4.4 \times 10^{-5}$; three clusters) and anger > neutral (with CAG repeat length correction, $P < 1 \times 10^{-10}$; six clusters) contrasts. Similar results were seen with probability of manifest disease onset within 5 years replacing CAG repeat length in the model. Regions in which the subjects with pre-manifest Huntington's disease had greater activation than the controls were seen in the happiness > neutral contrast after adjusting for probability of manifest disease onset within 5 years ($P = 4.0 \times 10^{-5;}$ three clusters); the effect was not seen after adjusting for CAG repeat length.

The network of increased activation in the subjects with pre-manifest Huntington's disease identified in the disgust > neutral contrast after CAG repeat length adjustment included bilateral middle frontal gyri and right pallidum.

The network of increased activation in the subjects with pre-manifest Huntington's disease identified in the anger > neutral contrast after CAG repeat length adjustment included right superior and left inferior frontal gyri, bilateral anterior cingulate cortex, left isthmus, right pons and right cerebellum.

The network of increased activation in the subjects with pre-manifest Huntington's disease identified in the happiness > neutral contrast after probability of manifest disease onset within 5 years adjustment included bilateral middle frontal gyri and left anterior cingulate cortex.

Activations did not differ significantly between the pre-manifest Huntington's disease and healthy control groups when CAG repeat length/probability of manifest disease onset within 5 years-related heterogeneity in the pre-manifest Huntington's disease group was not corrected for (Table 2, Model 1). The beta values for all subjects (controls and pre-manifest Huntington's disease) in the disgust > neutral condition at a sample of voxels in which reduced mean BOLD signal was seen in the subjects with pre-manifest Huntington's disease are shown plotted against CAG repeat length and probability of manifest disease onset within 5 years in Fig. 3: this demonstrates the distribution of the mean BOLD signal across both subject groups, and the associations with CAG repeat length and probability of manifest disease onset within 5 years in the pre-manifest Huntington's disease group, illustrating how these associations account for a significant level of variance.

(ii) Models testing for modulation in pre-manifest Huntington's disease activation by gene dosage (not including Ekman 60 regressor)

For the disgust > neutral contrast in the pre-manifest Huntington's disease group, both CAG repeat length and probability of manifest disease onset within 5 years covariates were

Table 3 Functional MRI results

Emotion and model number	Model description	Set level *P*-value	Number of clusters		Basal ganglia				Frontal lobe					Parietal lobe				Temporal lobe										Occipital lobe					Cingulate cortex				Cerebellum and pons		
					caudate	putamen	pallidum	thalamus	superior frontal gyrus	middle frontal gyrus	inferior frontal gyrus	precentral gyrus	paracentral lobule	postcentral gyrus	superior parietal lobule	inferior parietal lobule	precuneus	anterior insula	mid-insula	posterior insula	operculum	hippocampus	parahippocampal gyrus	superior temporal gyrus	middle temp gyrus	inferior temporal gyrus	lingual gyrus	cuneus	superior occipital gyrus	middle occipital gyrus	inferior occipital gyrus	anterior	middle	posterior	isthmus	anterior lobe of cerebellum	posterior lobe of cerebellum	pons
Disgust; model 2	Control > HD (with CAG adjustment)	$<1\times10^{-10}$	9	L								✓	✓		✓	✓		✓	✓																			
				R						✓			✓	✓																			✓					
Happiness; model 2	Control > HD (with CAG adjustment)	$<1x10^{-10}$	11	L	✓												✓				✓						✓		✓		✓							
				R	✓													✓	✓										✓		✓							
Anger; model 2	Control > HD (with CAG adjustment)	$<1x10^{-10}$	9	L									✓					✓	✓			✓							✓									
				R	✓													✓	✓			✓										✓					
Disgust; model 2	HD > Control (with CAG adjustment)	$4.4x10^{-5}$	3	L						✓																											
				R			✓			✓																											
Anger; model 2	HD > Control (with CAG adjustment)	$<1x10^{-10}$	6	L							✓																				✓			✓			
				R					✓																						✓				✓	✓
Disgust; model 3	HD only, negative correlation with CAG	$<1x10^{-10}$	21	L		✓						✓		✓	✓		✓	✓	✓											✓							
				R		✓	✓	✓		✓		✓					✓	✓	✓		✓									✓		✓			✓			
Happiness; model 3	HD only, negative correlation with CAG	$<1x10^{-10}$	7	L										✓																							
				R					✓					✓				✓	✓											✓			✓					
Disgust; model 3	HD only, positive correlation with CAG	$3.4x10^{-4}$	2	L																																	
				R							✓																											
Happiness; model 3	HD only, positive correlation with CAG	$<1x10^{-10}$	11	L					✓	✓										✓				✓	✓												✓
				R						✓															✓										✓		
Anger; model 3	HD only, positive correlation with CAG	$<1x10^{-10}$	7	L					✓		✓															✓						✓					
				R		✓			✓	✓																				✓							
Disgust; model 3	HD only, negative correlation with PDO	$<1x10^{-10}$	19	L						✓		✓		✓	✓		✓	✓	✓						✓		✓				✓	✓					
				R		✓	✓			✓						✓		✓	✓				✓				✓	✓	✓		✓	✓	✓		✓			
Happiness; model 3	HD only, negative correlation with PDO	$<1x10^{-10}$	9	L	✓																																
				R					✓			✓		✓	✓	✓		✓							✓							✓						
Happiness; model 3	HD only, positive correlation with PDO	$<1x10^{-10}$	6	L						✓																											✓
				R																		✓									✓					✓
Anger; model 3	HD only, positive correlation with PDO	$<1x10^{-10}$	6	L																		✓															
				R						✓			✓									✓							✓	✓							
Disgust; model 4	HD only, voxels in which BOLD signal was correlated with mean striatal BOLD signal (voxels with negative correlation between BOLD signal and CAG only)	$<1x10^{-10}$	21	L		✓				✓							✓		✓						✓	✓	✓		✓					✓			
				R		✓						✓		✓		✓	✓				✓							✓				✓						

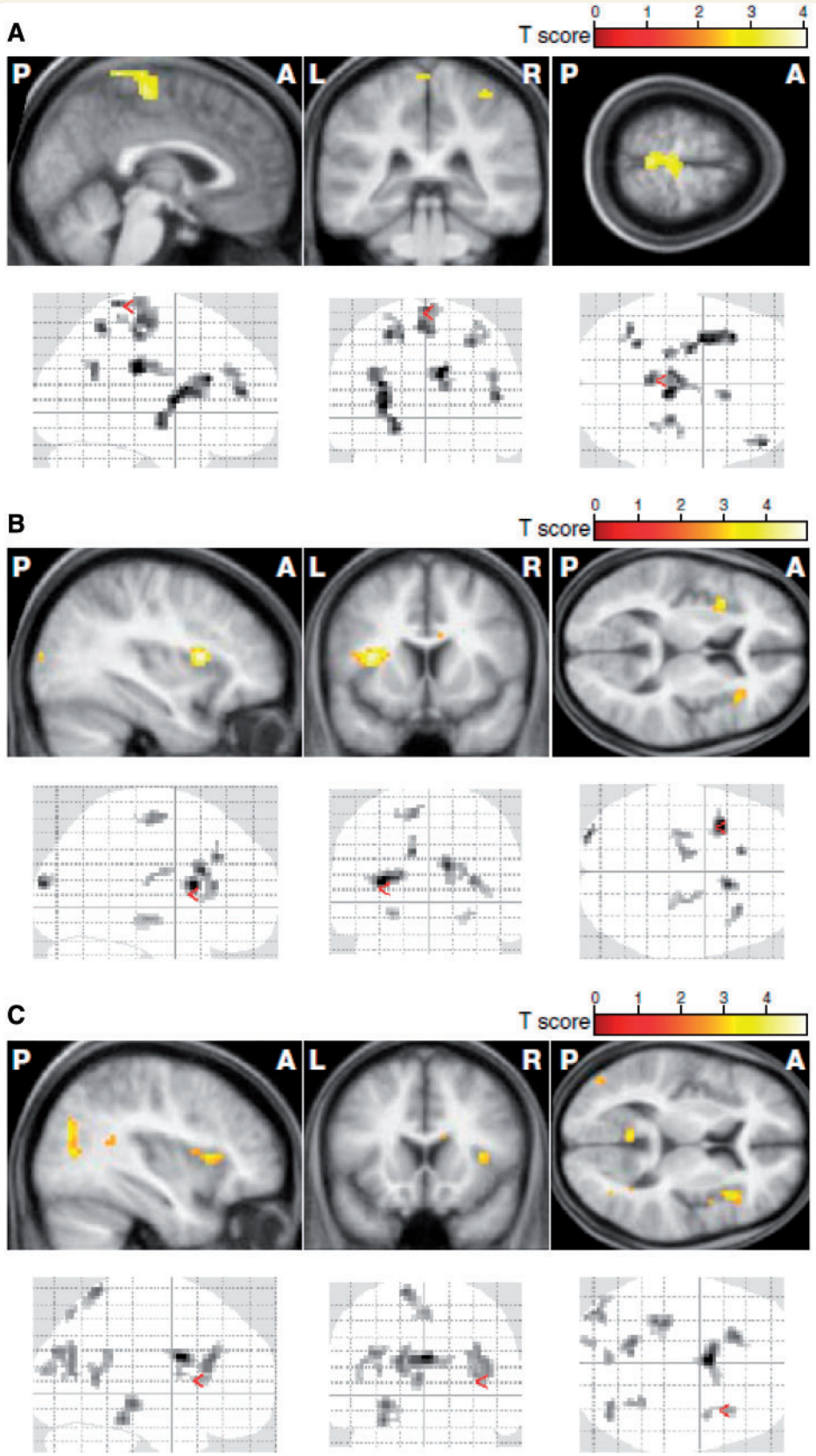

Figure 1 Statistical parametric maps showing the regions in which BOLD signal is lower in subjects with pre-manifest Huntington's disease than in controls after controlling for CAG repeat length in the following conditions: (**A**) disgust > neutral; (**B**) anger > neutral; and (**C**) happiness > neutral. P = posterior; A = anterior; L = left; R = right.

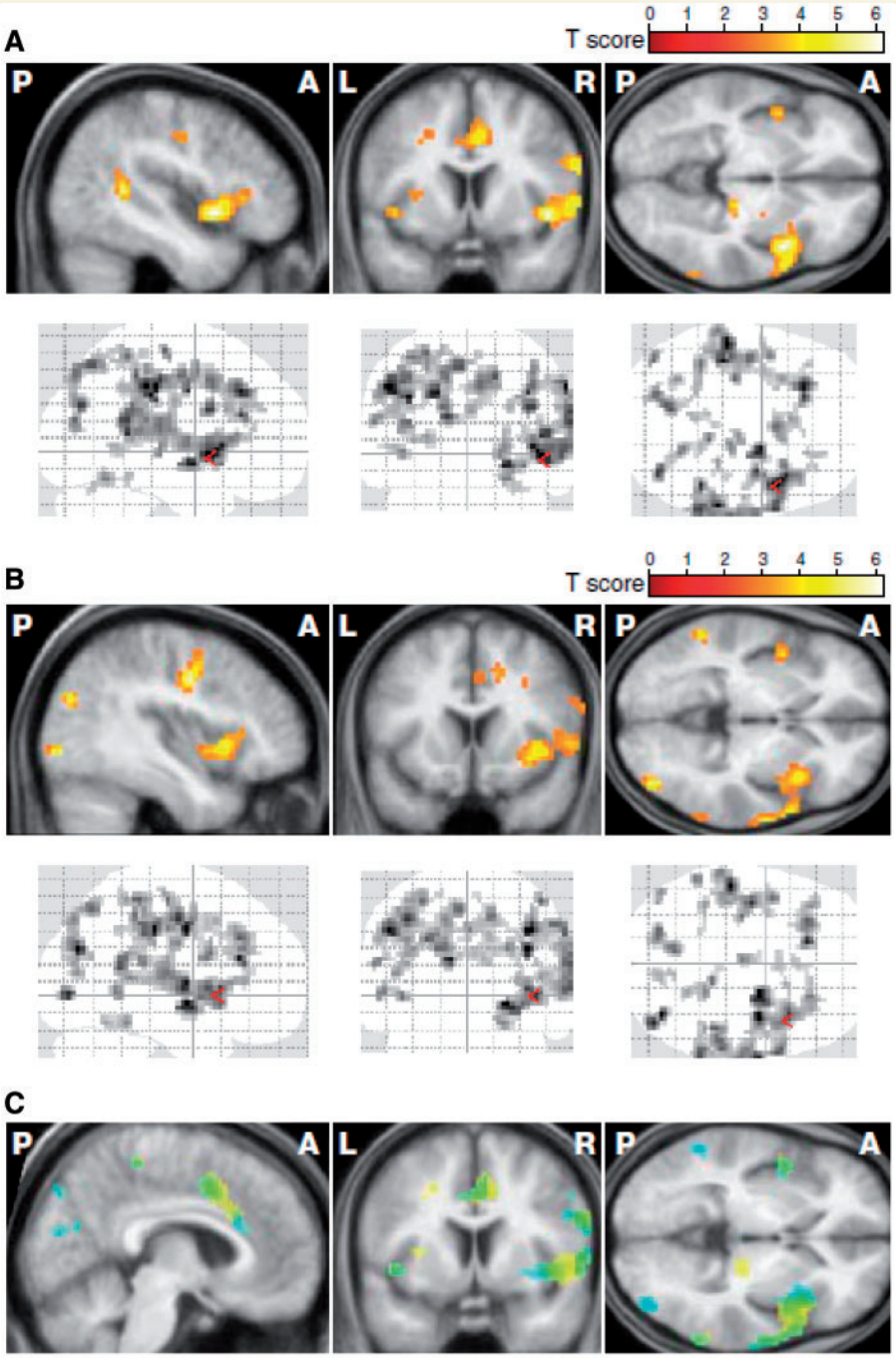

Figure 2 Statistical parametric maps showing the negative correlations between pre-manifest HD levels of BOLD in the disgust > neutral condition and: (**A**) CAG repeat length and (**B**) probability of manifest disease onset within five years. (**C**) shows the two sets of negative correlations on the same image: negative correlations with CAG repeat length are shown in yellow and negative correlations with probability of manifest disease onset within five years are shown in blue. Overlapping regions are shown in green. P = posterior; A = anterior; L = left; R = right.

inversely correlated with activation of an extensive network including bilateral anterior and mid-insulae and bilateral anterior and right mid-cingulate cortices, right middle frontal and middle occipital gyri, putamen, pallidum and anterior lobe of the cerebellum, and left precuneus, superior parietal lobule and pre- and postcentral gyri. CAG repeat length was additionally inversely correlated with activation of the right precuneus, precentral gyrus and thalamus, and left middle occipital gyrus and putamen. Probability of manifest disease onset within 5 years was additionally inversely correlated with activation of the left middle frontal gyrus, right superior and left inferior temporal gyri, right superior occipital gyrus, left angular gyrus, right inferior parietal lobule, bilateral cunei, and left mid- and right posterior cingulate cortices (Table 2, Model 3; Fig. 2).

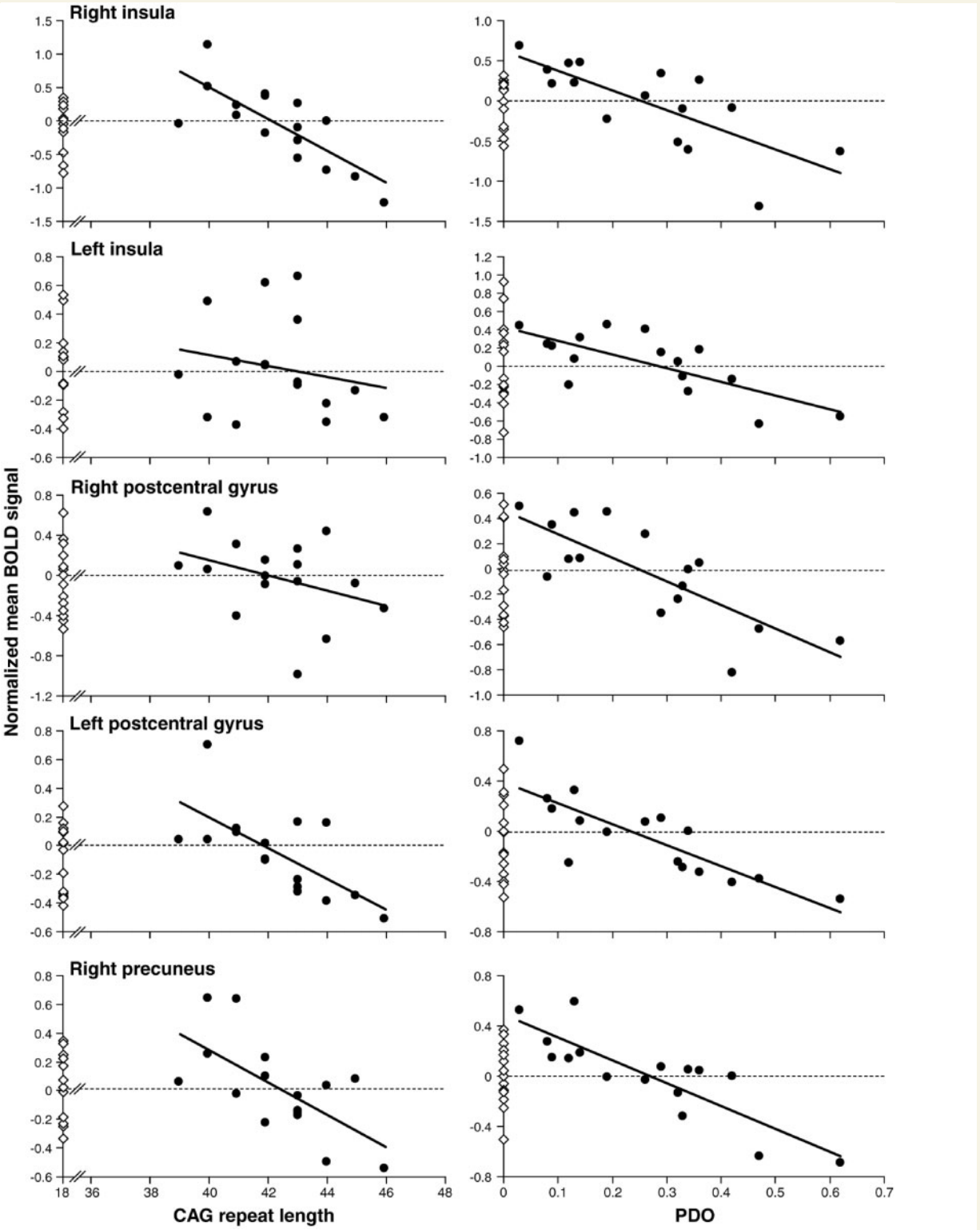

Figure 3 Plots of the normalized mean BOLD signal for each subject in the disgust > neutral contrast against CAG repeat length repeat length (*left*) and probability of disease onset in 5 years (*right*). Black circles represent subjects with pre-manifest Huntington's disease and white diamonds represent controls. Controls are plotted against a CAG repeat length repeat length of 18 based on a previous study showing a mean CAG repeat length repeat length of 18 in 360 controls (Snell *et al*., 1993), and a probability of manifest disease onset within 5 years of 0. PDO = probability of disease onset within 5 years.

For the happiness > neutral contrast in the pre-manifest Huntington's disease group, both the CAG repeat length and probability of manifest disease onset within 5 years covariates were inversely correlated with activation in the right superior frontal gyrus, right postcentral gyrus, right anterior insula, right middle occipital gyrus and right mid-cingulate cortex. CAG repeat length was additionally inversely correlated with activation of left postcentral gyrus and right mid-insula. Probability of manifest disease onset within 5 years was additionally inversely correlated with activation of the left caudate, right precentral gyrus, right superior and inferior parietal lobules and right middle temporal gyrus.

There were no significant correlations between CAG repeat length or probability of manifest disease onset within 5 years and BOLD level in the anger > neutral contrast.

We carried out further analyses to establish whether the predominantly extrastriatal correlations seen in the pre-manifest Huntington's disease group in the disgust > neutral contrast were driven by altered striatal activity. This contrast was chosen for additional analyses because the network it revealed was the most anatomically extensive of all our results. Mean BOLD signal within the striatal subregion covaried with neuronal activity in extrastriatal areas in the disgust > neutral contrast, including voxels within the right pre-and postcentral gyri, left middle frontal gyrus, right inferior parietal lobule, bilateral precunei and cunei, right operculum, left inferior temporal gyrus, left lingual gyrus, left middle occipital gyrus, right anterior cingulate gyrus and left anterior lobe of the cerebellum (Table 2, Model 4; Supplementary Fig. 5). However, this covariance between striatal and extrastriatal areas was not uniform: covariation was not observed in the anterior insulae, right mid-insula, left anterior or right mid-cingulate cortices, right middle frontal gyrus, right middle occipital gyrus, right anterior lobe of the cerebellum, left superior parietal lobule or left pre- or postcentral gyri.

(iii) Models testing for differences in activation between the pre-manifest Huntington's disease and control groups and including the Ekman 60 regressor

The activation profile in the disgust > neutral contrast had a stronger positive correlation with out-of-scanner disgust recognition performance in the pre-manifest Huntington's disease group than in healthy controls: this activation profile comprised distributed bihemispheric areas including mid-insulae and precentral gyri, as well as left putamen, left middle frontal gyrus, right postcentral gyrus, right superior parietal lobule, right superior temporal gyrus, left lingual gyrus, left anterior cingulate cortex and right anterior lobe of the cerebellum ($P < 1 \times 10^{-10}$; 14 clusters; Table 2, Model 5; Supplementary Fig. 6). The areas showing this correlation partly overlapped those areas (described in the section above) in which there was a negative correlation with CAG repeat length and probability of manifest disease onset within 5 years in the pre-manifest Huntington's disease group in the disgust > neutral contrast (Fig. 2).

The activation profile in the anger > neutral contrast had a stronger positive correlation with out-of-scanner anger recognition performance in the pre-manifest Huntington's disease group than in healthy controls in the right superior frontal gyrus, and left middle frontal and postcentral gyri ($P = 3.7 \times 10^{-5}$; three clusters; Table 2, Model 5). The activation profile had a stronger positive correlation with out-of-scanner anger recognition performance in the healthy controls in the left pallidum, left precuneus, right middle and left inferior occipital gyri ($P < 1 \times 10^{-10}$; six clusters; Table 2, Model 5).

These analyses were not carried out for the happiness > neutral condition because performance in the Ekman test for happiness recognition was at ceiling level for most subjects.

Structural: voxel-based morphometry

Voxel-based morphometry results are shown in Supplementary Table 4. On whole-brain analysis, the pre-manifest Huntington's disease group had lower grey matter volume than the control group in the caudate head and putamen bilaterally (right $P = 0.022$; left $P = 0.028$) and in the left occipital lobe ($P = 0.033$). No regions of higher grey matter volume were found in the pre-manifest Huntington's disease group compared with controls. Within the pre-manifest Huntington's disease group, grey matter volume in the caudate and putamen was negatively correlated with CAG repeat length (small volume-corrected with bilateral caudate/putamen/pallidum region of interest, $P \leqslant 0.01$; correlation with grey matter volume in left caudate and putamen only on whole-brain analyses, $P = 0.007$); and with probability of manifest disease onset within 5 years (whole-brain analysis, $P \leqslant 0.03$) (Supplementary Fig. 7). Within the reduced search volume defined by the bilateral caudate/putamen/pallidum/insula/amygdala/somatosensory cortex/orbital frontal cortex mask, grey matter volume in the left precentral gyrus, left middle frontal and right superior frontal gyri was negatively correlated with CAG repeat length, and grey matter volume in the left caudate head and putamen and right middle frontal gyrus was negatively correlated with probability of manifest disease onset within 5 years. There was no evidence for the reverse associations.

No significant interactions between subject group, grey matter volume and out-of-scanner emotion recognition performance were found for out-of-scanner disgust or anger recognition performance, irrespective of whether CAG repeat length and probability of manifest disease onset within 5 years were included as 'nuisance covariates' (happiness was not evaluated because performance was at ceiling for most subjects).

Discussion

Here we have shown that viewing facial expressions of anger, disgust or happiness is associated with altered levels of neural activation in individuals with pre-manifest Huntington's disease in comparison with healthy control subjects. In the subjects with pre-manifest Huntington's disease, significantly lower levels of neural activation were present in a distributed brain network; more anatomically limited regions of increased activation were present, primarily in the frontal lobes. Huntington's disease-associated activation differences were not restricted to a particular emotional expression or emotion valence. Furthermore, this differential activation profile varied amongst individual subjects with pre-manifest Huntington's disease and was observed only after

controlling for effects from Huntington's disease genotype (CAG repeat length repeat length/probability of manifest disease onset within 5 years). Huntington's disease, including pre-manifest Huntington's disease, appears to be a remarkably heterogeneous condition with extensive variation in phenotype between individuals. It is therefore perhaps unsurprising that (i) we found extensive variation in neural activity within the pre-manifest Huntington's disease group; and that (ii) the differential activation between the subjects with pre-manifest Huntington's disease and controls was only seen once the variance associated with CAG repeat length/probability of disease onset within 5 years was explicitly modelled. The overall relationship in the pre-manifest Huntington's disease group between Huntington's disease gene status and neural activity was complex. Differential activation relative to controls occurred independently of gene dosage during processing of all three tested emotions, arguing for a baseline alteration in neural activity conferred by the expanded Huntington's disease gene; however, associations between gene dosage (CAG repeat length/probability of manifest disease onset within 5 years) and BOLD signal were also seen, suggesting a genetic dose-dependent reduction in neural activity. Previous functional MRI studies (Paulsen *et al*., 2004; Wolf *et al*., 2007; Zimbelman *et al*., 2007; Saft *et al*., 2008; Kloppel *et al*., 2009*a*) have shown that pre-manifest Huntington's disease gene carriers relative to healthy controls exhibit either an overall increase in BOLD signal or an 'inverted U'-like pattern of change over time. Considered in conjunction with this previous work, our findings suggest that the profile of Huntington's disease-associated changes in BOLD signal may be specific to a particular cognitive process or may follow a different time course for different cognitive functions.

Negative correlations were observed here in the pre-manifest Huntington's disease group between striatal and extrastriatal regional BOLD signal, and between BOLD signal, Huntington's disease gene status and CAG repeat length and probability of manifest disease onset within 5 years in widespread cortical areas. The covariance of striatal and extrastriatal activity was not uniform across brain regions; this suggests that the modulation of extrastriatal activity is not entirely driven by modulation of striatal activity. Positive correlations between BOLD signal, Huntington's disease gene status and CAG repeat length and probability of manifest disease onset within 5 years were observed in a more anatomically limited distribution—most consistently in the superior and middle frontal gyri—suggesting a predominantly frontal, compensatory network. Huntington's disease-associated functional changes were more anatomically extensive than structural (voxel-based morphometry) changes: while indirect comparisons of the statistical inferences drawn from separate models of different imaging modalities must be cautious, the present findings suggest that altered extrastriatal function occurs at an early stage in the pathogenesis of Huntington's disease and in the absence of detectable equivalent extrastriatal volume loss. The finding of modulated neural activity in widespread brain regions extends the previous observation of reduced insula activation using a similar functional MRI paradigm (Hennenlotter *et al*., 2004), perhaps reflecting our larger subject cohort with enhanced power to carry out less anatomically constrained analyses. Three structural imaging studies to date have assessed the relationship between regional brain volumes and accuracy of explicit classification of facial expressions of emotion in Huntington's disease. The largest of these found no correlation between emotion recognition performance and caudate volumes (Johnson *et al*., 2007), while correlations have been shown with regional grey matter volume in other brain areas, including anteroventral insula (disgust) (Kipps *et al*., 2007), amygdala (happiness) (Kipps *et al*., 2007) and striatum (anger) (Henley *et al*., 2008). Allowing for the important caveats of methodological variation and intrinsic biological heterogeneity, our findings suggest a potential unifying explanation for these apparent disparities in previous work: Huntington's disease modulates activity across a predominantly extrastriatal but distributed emotion processing network.

Considerable interest in the literature on clinical Huntington's disease has centred on the specificity of deficits for the processing of particular emotions; no definitive synthesis has emerged (Henley *et al*., 2011). Huntington's disease-associated variability in emotion processing is in keeping with the marked heterogeneity of Huntington's disease symptom expression in general: study of emotion processing in Huntington's disease is therefore a useful window onto the phenotypical heterogeneity of the disease. In the present study, individual emotions were associated with separable profiles of functional alteration, suggesting that the mechanism of Huntington's disease-associated modulation may be at least partly emotion-specific. Facial expressions of positive emotion (i.e. happiness) are intrinsically easier to recognize than negative emotions, at least using conventional emotion stimuli; a smile is both highly distinctive and pathognomonic of happiness (Adolphs, 2002), whereas negative emotions (such as anger and disgust) rely on more fine-grained encoding across a broader range of distinctive emotion categories. Healthy subjects typically perform at ceiling level for recognition of happy facial expressions and, indeed, after accounting for this, a behavioural impairment in the recognition of happy facial expressions has not been reported in pre-manifest Huntington's disease. In the present study, we have shown that functional responses to expressions of happiness as well as negative emotions (anger and disgust) are altered in pre-manifest Huntington's disease despite a level of out-of-scanner recognition accuracy comparable to healthy individuals. These findings suggest that functional MRI indices may be more sensitive than behavioural indices in tracking altered emotion processing in Huntington's disease, and raise the further possibility that the use of alternative, more finely differentiated stimuli might however reveal hitherto largely undetected deficits in processing positive-valence facial expressions. The detection of impaired recognition of vocal expressions of positive emotions in Huntington's disease in one previous study (Robotham *et al*., 2011) supports this assertion.

In the present task we sought to minimize the requirement for in-scanner explicit recognition or labelling of particular emotions as this is one potential source of discrepancy between past studies of emotion processing in Huntington's disease (Snowden *et al*., 2008). Although debriefing of our subjects revealed that all became aware of the emotional content of the stimuli, this was not reflected in any systematic trend in BOLD response. It is therefore unlikely that the differential associations we observed in

pre-manifest Huntington's disease simply reflect altered labelling of facial emotions. Rather, we argue that these Huntington's disease-associated activation changes reflect altered brain mechanisms intrinsic to the processing of emotional stimuli: differential neural associations for the processing of particular emotions could arise if (as is likely) the pathological process in Huntington's disease affects the brain substrates for processing particular emotions non-uniformly as the disease develops. The inclusion of individuals at different stages of disease evolution is a potential source of discrepancy between this and other studies of emotion processing in Huntington's disease (Snowden *et al*., 2008; Henley *et al*., 2011), and the variance in our functional MRI data underlines the importance of considering this factor.

Our results suggest that a distributed cortico-striatal network modulates the processing of emotional stimuli in pre-manifest Huntington's disease. There are several possible mechanisms that could mediate this modulatory effect. The insula has been implicated previously as a key region associated with disgust processing (Phillips *et al*., 1997; Wicker *et al*., 2003, Harrison *et al*., 2010); though the precise role of this area remains unclear, it may facilitate emotion imagery or the processing of emotion under conditions of increased cognitive load (Phan *et al*., 2002). The somatosensory cortices have also been implicated in emotion recognition (Adolphs *et al*., 2000; Banissy *et al*., 2010) and may at least partly facilitate understanding of the emotional states of others via a mimicry process (Adolphs *et al*., 2000). Impaired ability to internalize an observed emotional state through disordered somatosensory representations might plausibly accompany the evolving disease process in Huntington's disease. The precuneus has also been implicated in emotion recognition (Ochsner *et al*., 2004); however, it has also consistently been shown to be active in resting state functional MRI studies. Resting state studies reveal the 'default mode network': those regions of the brain implicated in mind-wandering, or day-dreaming (Mason *et al*., 2007). Modulation of activity of these 'default mode' areas in this study might indicate that increased neural resources are directed toward emotion processing (i.e. the processing of salient external stimuli) as pre-manifest Huntington's disease subjects approach disease onset and inhibit day-dreaming to focus attention on the task. The middle frontal gyri, in which we detected increased neural activity in our subjects with pre-manifest Huntington's disease, are often activated in tasks requiring executive functions, such as response inhibition (Blasi *et al*., 2006) and attentional control (Corbetta and Shulman, 2002). A compensatory increase in executive processing of affective stimuli is a credible mechanism by which normal emotion recognition ability might be retained in the face of reduced neural activity in other emotion processing brain regions in pre-manifest Huntington's disease.

This study has demonstrated modulation of a large-scale, predominantly extrastriatal functional brain network in association with the processing of positive and negative emotions in pre-manifest Huntington's disease gene-carriers compared with healthy control subjects. Neural activation during emotion processing was associated with metrics of Huntington's disease gene dosage. These functional alterations in the pre-manifest Huntington's disease cohort were not reflected in an overall behavioural deficit in out-of-scanner emotion recognition, nor modified substantially by incorporation of emotion recognition performance as a regressor in the BOLD analysis; behavioural interpretations of the functional MRI findings must, therefore, be cautious. There was, however, evidence for increased strength of association between neural activation and recognition performance in the pre-manifest Huntington's disease group compared with controls, and for modulation of emotion recognition performance by gene dosage. These findings strongly suggest that the functional alterations identified here are behaviourally relevant. The functional alterations extended widely beyond the region of structural brain atrophy; furthermore, structural associations of emotion processing were not identified in this pre-manifest Huntington's disease cohort. Taken together, the present findings suggest that pathophysiological metrics of emotion processing may have a role as biomarkers of early (pre-manifest) Huntington's disease, particularly in the assessment of extrastriatal dysfunction. The results further suggest that metrics of extrastriatal function should be pursued and exploited in designing and assessing new symptomatic and disease-modifying therapies in Huntington's disease. Quantification of resting state regional cerebral blood flow has recently been proposed as a biomarker in Huntington's disease (Wolf *et al*., 2011); future longitudinal studies could helpfully explore the potential of task-based functional MRI to complement resting state data. Key directions for future work will include the detailed longitudinal tracking of functional in relation to structural and behavioural change in Huntington's disease (including studies expressed designed to compare the sensitivity of structural and functional imaging modalities), and assessment of a wider range of emotional stimuli and relevant in-scanner behavioural tasks.

Acknowledgements

The authors wish to thank the pre-manifest gene carriers and controls who generously gave their time to do this study. The authors also wish to thank the reviewers of our manuscript for their helpful comments, and Drs John Ashburner and Guillaume Flandin for methodological advice, Dr Rachael Scahill for critical review of the manuscript and Ray Young for his assistance with the figures.

Funding

This work was funded by a grant from the Wellcome Trust to R.S.J.F. (PI) and S.J.T. (Ref 075696/Z/04/Z). The work in S.J.T.'s lab is also funded by grants from the MRC, NIHR, CHDI Foundation, Euro-HD Network, EU FP7 Health programme, UK HD association and the Brain Research Trust. JDW is supported by a Wellcome Trust Senior Clinical Fellowship. The Wellcome Trust Centre for Neuroimaging is supported by core funding from the Wellcome Trust 091593/Z/10/Z. The Dementia Research Centre is an Alzheimer's Research Trust Co-ordinating Centre and has also received equipment funded by the Alzheimer's Research Trust. This work was undertaken at UCLH/

UCL who acknowledge support from the respective Department of Health's NIHR Biomedical Research Centres.

Supplementary material

Supplementary material is available at *Brain* online.

References

Unified Huntington's Disease Rating Scale: reliability and consistency. Huntington Study Group. Mov Disord 1996; 11: 136–42.

Adolphs R. Recognizing emotion from facial expressions: psychological and neurological mechanisms. Behav Cogn Neurosci Rev 2002; 1: 21–62.

Adolphs R. Neural systems for recognizing emotion. Curr Opin Neurobiol 2001; 12: 169–77.

Adolphs R, Damasio H, Tranel D, Cooper G, Damasio AR. A role for somatosensory cortices in the visual recognition of emotion as revealed by three-dimensional lesion mapping. J Neurosci 2000; 20: 2683–90.

Ashburner J. A fast diffeomorphic image registration algorithm. Neuroimage 2007; 38: 95–113.

Ashburner J, Friston FJ. Unified segmentation. Neuroimage 2005; 26: 839–51.

Ashburner J, Friston KJ. Voxel-based morphometry-the methods. Neuroimage 2000; 11 (6 Pt 1): 805–21.

Aviezer H, Bentin S, Hassin RR, Meschino WS, Kennedy J, Grewal S, et al. Not on the face alone: perception of contextualized face expressions in Huntington's disease. Brain 2009; 132: 1633–44.

Aylward EH, Brandt J, Codori AM, Mangus RS, Barta PE, Harris GJ. Reduced basal ganglia volume associated with the gene for Huntington's disease in asymptomatic at-risk persons. Neurology 1994; 44: 823–8.

Banissy MJ, Sauter DA, Ward J, Warren JE, Walsh V, Scott SK. Suppressing sensorimotor activity modulates the discrimination of auditory emotions but not speaker identity. J Neurosci 2010; 30: 13552–7.

Benton AL, Hamsher KS, Varney N, Spreen O. Contributions to neuropsychological assessment: A clinical manual. Oxford: Oxford University Press; 1983.

Blasi G, Goldberg TE, Weickert T, Das S, Kohn P, Zoltick B, et al. Brain regions underlying response inhibition and interference monitoring and suppression. Eur J Neurosci 2006; 23: 1658–64.

Borkowski JG, Benton AL, Spreen O. Word fluency and brain damage. Neuropsychologia 1967; 5: 135–40.

Butters N, Granholm E, Salmon DP, Grant I, Wolfe J. Episodic and semantic memory: a comparison of amnesic and demented patients. J Clin Exp Neuropsychol 1987; 9: 479–97.

Calder A, Keane J, Young A, Lawrence A, Mason S, Barker R. The relation between anger and different forms of disgust: implications for emotion recognition impairments in Huntington's disease. Neuropsychologia 2010; 48: 2719–29.

Corbetta M, Shulman GL. Control of goal-directed and stimulus-driven attention in the brain. Nat Rev Neurosci 2002; 3: 201–15.

Deichmann R. Fast structural brain imaging using an MDEFT sequence with a FLASH-EPI hybrid readout. Neuroimage 2006; 33: 1066–71.

Friston KJ, Holmes A, Poline J-B, Price CJ, Frith CD. Detecting activations in PET and fMRI: levels of inference and power. Neuroimage 1996; 4 (3 Pt 1): 223–35.

Friston KJ, Holmes AP, Worsley KJ, Poline J-P, Frith CD, Frackowiak RSF. Statistical parametric maps in functional imaging: a general linear approack. Hum Brain Mapp 1995; 2: 189–210.

Gray JM, Young AW, Barker WA, Curtis A, Gibson D. Impaired recognition of disgust in Huntington's disease gene carriers. Brain 1997; 120 (Pt 11): 2029–38.

Harrison NA, Gray MA, Gianaros PJ, Critchley HD. The Embodiment of Emotional Feelings in the Brain. J Neurosci 2010; 30: 12878.

Hayasaka S, Phan KL, Liberzon I, Worsley KJ, Nichols TE. Nonstationary cluster-size inference with random field and permutation methods. Neuroimage 2004; 22: 676–87.

Henley SMD, Novak MJU, Frost C, King J, Tabrizi SJ, Warren JD. Emotion recognition in Huntington's disease: a systematic review. Neurosci Biobehav Rev 2011; 36: 237–53.

Henley SM, Wild EJ, Hobbs NZ, Frost C, MacManus DG, Barker RA, et al. Whole-brain atrophy as a measure of progression in premanifest and early Huntington's disease. Mov Disord 2009; 24: 932–6.

Henley SM, Wild EJ, Hobbs NZ, Warren JD, Frost C, Scahill RI, et al. Defective emotion recognition in early HD is neuropsychologically and anatomically generic. Neuropsychologia 2008; 46: 2152–60.

Hennenlotter A, Schroeder U, Erhard P, Haslinger B, Stahl R, Weindl A, et al. Neural correlates associated with impaired disgust processing in pre-symptomatic Huntington's disease. Brain 2004; 127 (pt 6): 1446–53.

Johnson SA, Stout JC, Solomon AC, Langbehn DR, Aylward EH, Cruce CB. Beyond disgust: impaired recognition of negative emotions prior to diagnosis in Huntington's disease. Brain 2007; 130 (Pt 7): 1732–44.

Kipps CM, Duggins AJ, McCusker EA, Calder AJ. Disgust and happiness recognition correlate with anteroventral insula and amygdala volume respectively in preclinical Huntington's disease. J Cogn Neurosci 2007; 19: 1206–17.

Kloppel S, Draganski B, Siebner HR, Tabrizi SJ, Weiller C, Frackowiak RS. Functional compensation of motor function in pre-symptomatic Huntington's disease. Brain 2009a; 132 (Pt 6): 1624–32.

Kloppel S, Stonnington CM, Petrovic P, Mobbs D, Tuscher O, Craufurd D, et al. Irritability in pre-clinical Huntington's disease. Neuropsychologia 2009b; 48: 549–57.

Langbehn DR, Brinkman RR, Falush D, Paulsen JS, Hayden MR. A new model for prediction of the age of onset and penetrance for Huntington's disease based on CAG length. Clin Genet 2004; 65: 267–77.

Maldjian JA, Laurienti PJ, Burdette JH. Precentral gyrus discrepancy in electronic versions of the Talairach atlas. Neuroimage 2004; 21: 450–5.

Maldjian JA, Laurienti PJ, Kraft RA, Burdette JH. An automated method for neuroanatomic and cytoarchitectonic atlas-based interrogation of fMRI data sets. Neuroimage 2003; 19: 1233–9.

Mason M, Norton M, Van Horn J, Wegner D, Grafton S, Macrae C. Wandering minds: the default network and stimulus-independent thought. Science 2007; 315: 393.

Montagne B, Kessels RP, Kammers MP, Kingma E, de Haan EH, Roos RA, et al. Perception of emotional facial expressions at different intensities in early-symptomatic Huntington's disease. Eur Neurol 2006; 55: 151–4.

Nelson HE, Willison J. The National Adult reading Test, 2nd edn. Windsor, UK: NFER-Nelson; 1991.

Novak MJU, Tabrizi SJ. Huntington's disease. BMJ 2010; 340: c3109.

Ochsner K, Knierim K, Ludlow D, Hanelin J, Ramachandran T, Glover G, et al. Reflecting upon feelings: an fMRI study of neural systems supporting the attribution of emotion to self and other. J Cogn Neurosci 2004; 16: 1746–72.

Paulsen JS, Zimbelman JL, Hinton SC, Langbehn DR, Leveroni CL, Benjamin ML, et al. fMRI biomarker of early neuronal dysfunction in presymptomatic Huntington's Disease. Am J Neuroradiol 2004; 25: 1715–21.

Paulsen JS, Hayden M, Stout JC, Langbehn DR, Aylward E, Ross CA, et al. Preparing for preventive clinical trials: the Predict-HD study. Arch Neurol 2006; 63: 883–90.

Phan KL, Wager T, Taylor SF, Liberzon I. Functional neuroanatomy of emotion: a meta-analysis of emotion activation studies in PET and fMRI. Neuroimage 2002; 16: 331–48.

Phillips ML, Young AW, Senior C, Brammer M, Andrew C, Calder AJ, et al. A specific neural substrate for perceiving facial expressions of disgust. Nature 1997; 389: 495–8.

Reading SA, Dziorny AC, Peroutka LA, Schreiber M, Gourley LM, Yallapragada V, et al. Functional brain changes in presymptomatic Huntington's disease. Ann Neurol 2004; 55: 879–83.

Robotham L, Sauter DA, Bachoud-Levi A-C, Trinkler I. The impairment of emotion recognition in Huntington's disease extends to positive emotions. Cortex 2011; 47: 880–4.

Rosas HD, Koroshetz WJ, Chen YI, Skeuse C, Vangel M, Cudkowicz ME. Evidence for more widespread cerebral pathology in early HD: an MRI-based morphometric analysis. Neurology 2003; 60: 1615–20.

Saft C, Schuttke A, Beste C, Andrich J, Heindel W, Pfleiderer B. fMRI reveals altered auditory processing in manifest and premanifest Huntington's disease. Neuropsychologia 2008; 46: 1279–89.

Smith A. The Symbol Digit Modalities Test: a neuropsychologic test for economic screening of learning and other cerebral disorders. Learning Disorders 1968; 3: 83–91.

Snell RG, MacMillan JC, Cheadle JP, Fenton I, Lazarou LP, Davies P, et al. Relationship between trinucleotide repeat expansion and phenotypic variation in Huntington's disease. Nat Genet 1993; 4: 393–7.

Snowden JS, Austin NA, Sembi S, Thompson JC, Craufurd D, Neary D. Emotion recognition in Huntington's disease and frontotemporal dementia. Neuropsychologia 2008; 46: 2638–49.

Sprengelmeyer R, Schroeder U, Young AW, Epplen JT. Disgust in pre-clinical Huntington's disease: a longitudinal study. Neuropsychologia 2006; 44: 518–33.

Sprengelmeyer R, Young AW, Calder AJ, Karnat A, Lange H, Homberg V, et al. Loss of disgust. Perception of faces and emotions in Huntington's disease. Brain 1996 Oct; 119 (Pt 5):1647–65.

Stroop JR. Studies of interference in serial verbal reactions. J Exp Psychol 1935; 18: 643–62.

Tabrizi SJ, Langbehn DR, Leavitt BR, Roos RA, Durr A, Craufurd D, et al. Biological and clinical manifestations of Huntington's disease in the longitudinal TRACK-HD study: cross-sectional analysis of baseline data. Lancet Neurol 2009; 8: 791–801.

Thieben MJ, Duggins AJ, Good CD, Gomes L, Mahant N, Richards F, et al. The distribution of structural neuropathology in pre-clinical Huntington's disease. Brain 2002; 125 (Pt 8): 1815–28.

Vonsattel JP, Myers RH, Stevens TJ, Ferrante RJ, Bird ED, Richardson EP Jr. Neuropathological classification of Huntington's disease. J Neuropathol Exp Neurol 1985; 44: 559–77.

Wang K, Hoosain R, Yang RM, Meng Y, Wang CQ. Impairment of recognition of disgust in Chinese with Huntington's or Wilson's disease. Neuropsychologia 2003; 41: 527–37.

Weiskopf N, Hutton C, Josephs O, Deichmann R. Optimal EPI parameters for reduction of susceptibility-induced BOLD sensitivity losses: A whole-brain analysis at 3 T and 1.5 T. Neuroimage 2006; 33: 493–504.

Wicker B, Keysers C, Plailly J, Royet J, Gallese V, Rizzolatti G. Both of us disgusted in my insula:: the common neural basis of seeing and feeling disgust. Neuron 2003; 40: 655–64.

Wolf RC, Vasic N, Schonfeldt-Lecuona C, Landwehrmeyer GB, Ecker D. Dorsolateral prefrontal cortex dysfunction in presymptomatic Huntington's disease: evidence from event-related fMRI. Brain 2007; 130: 2845–57.

Wolf RC, Sambataro F, Vasic N, Schonfeldt-Lecuona C, Ecker D, Landwehrmeyer B. Altered frontostriatal coupling in pre-manifest Huntington's disease: effects of increasing cognitive load. Eur J Neurol 2008; 15: 1180–90.

Wolf RC, Gron G, Sambataro F, Vasic N, Wolf ND, Thomann PA, et al. Magnetic resonance perfusion imaging of resting-state cerebral blood flow in preclinical Huntington's disease. J Cereb Blood Flow Metab 2011; 31: 1908–18.

Worsley KJ, Marrett S, Neelin P, Vandal AC, Friston KJ, Evans AC. A unified statistical approach for determining significant signals in images of cerebral activation. Hum Brain Mapp 1996; 4: 58–73.

Young AW, Perrett DI, Calder AJ, Sprengelmeyer R, Ekman P. Facial expressions of emotion: stimuli and tests (FEEST). Psychology 2002. Thames Valley Test Company.

Zimbelman JL, Paulsen JS, Mikos A, Reynolds NC, Hoffmann RG, Rao SM. fMRI detection of early neural dysfunction in preclinical Huntington's disease. J Int Neuropsychol Soc 2007; 13: 758–69.